Hindawi
Shock and Vibration
Volume 2019, Article ID 4535072, 11 pages
https://doi.org/10.1155/2019/4535072

Research Article

Damping Multimode Switching Control of Semiactive Suspension for Vibration Reduction in a Wheel Loader

Tao Wei [1,2] **and Liu Zhiqiang** [1]

[1] *School of Automotive and Traffic Engineering, Jiangsu University, Zhenjiang 212013, China*
[2] *Jiangsu Jiaotong College, Zhenjiang 212028, China*

Correspondence should be addressed to Tao Wei; xi16898168@126.com

Received 25 September 2018; Revised 28 January 2019; Accepted 12 February 2019; Published 21 March 2019

Academic Editor: Roger Serra

The aim of this work is the control design and analysis of a semiactive axle suspension system for vibration reduction in a wheel loader. Unlike a traditional semiactive suspension system with continuously adjustable shock absorber, in this work, a novel axle suspension with multiple damping modes is proposed for the wheel loader. The multimode switching damping characteristics are achieved by just changing the discrete statuses of two high-speed switch electromagnetic valves, which makes the damping adjustment simpler and more reliable. However, because of the existence of discrete events, i.e., the on-off statuses of switch electromagnetic valves, the axle suspension proposed for the wheel loader poses a challenging hybrid control problem. To solve this problem, the mixed logical dynamical (MLD) modeling approach for hybrid systems is applied to model the dynamic characteristics of the system damping control procedure. Using this model, a hybrid model predictive control (HMPC) strategy is further designed, which can determine the optimal switching sequences of the discrete damping modes according to the axle suspension performance indices. Finally, to verify the effectiveness of the proposed semiactive axle suspension with multiple damping modes and its control approach, simulation analyses are conducted.

1. Introduction

Because of the high working efficiency, good flexibility, and convenient operation, wheel loaders are often used in the construction and mining fields [1, 2]. However, because the wheel loader often needs to be worked under off-road conditions, continuous exposure to the strong vibration caused by uneven road will reduce working efficiency and damage the drivers' health [3]. In addition, unlike ordinary road vehicles, the wheel loader is often manufactured without any axle suspensions, i.e., the front and rear wheels are attached directly to the body, which make it experience severe vibration and poor stability. Therefore, to reduce the vibration transmitted to the driver, the design of advanced vibration isolation system for the wheel loader is necessary [4, 5]. According to the research results of relevant literatures, the most efficient way to reduce vehicle vibrations is to design the fully suspended wheel axles [6, 7]. In [8], the dynamic behaviors of wheel loaders with different layouts of hydropneumatic suspensions are investigated, and the research results show that the axle suspensions can help the body vertical acceleration to be reduced. In [9], a wheel loader with and without axle suspensions is modeled using multibody system dynamics, and the effect of introducing axle suspension on wheel loader ride comfort is also investigated.

As is known to all, different types of suspension systems have significant differences in performance and cost [10]. The passive suspension has the advantages of simple structure and low cost, but the space for vibration isolation performance improvement is limited due to the lack of adaptability [11]. The active suspension can significantly improve the vehicle dynamical performance by controlling the actuator force directly, but high cost and energy consumption are the main factors restricting its development [12]. Through comprehensive consideration, the semiactive

suspension can provide a very good compromise between cost and performance, which makes it become the research hotspots in the suspension field [13–15]. According to the literature reports about the semiactive suspension system, the damping adjustment is often achieved by using a continuously adjustable shock absorber with different types of regulating mechanisms [16–18]. It is obvious that these types of shock absorbers have relatively complex structure and are difficult to control. In addition, some experimental results have shown that the performance of semiactive suspension cannot be influenced significantly by small damping variations [19]. Therefore, to achieve better compromise between cost and performance for the semiactive suspension, the shock absorber with multiple damping modes achieved by the simple and reliable regulating mechanism may be more appropriate [20].

Compared with the traditional semiactive suspension system with continuously adjustable shock absorber, the aim of this work is to design a new semiactive axle suspension with multiple damping modes for the wheel loader. The multimode switching damping characteristics are achieved by just changing the discrete statuses of two high-speed switch electromagnetic valves, which make the oil flow paths change during the piston moving up and down. This means that the controller designed for the new semiactive axle suspension must obtain the optimal switching sequences of the discrete damping modes by considering the suspension performance requirements. Note that since the statuses of the high-speed switch electromagnetic valves are typical discrete events, the damping control process of the new semiactive axle suspension proposed for the wheel loader can then be regarded as a class of hybrid systems. Therefore, to achieve the effective control of the proposed axle suspension with multiple damping modes, the control methods based on hybrid systems should be applied.

Over the past few decades, to describe those systems, which contain both continuous dynamical processes and discrete variables, hybrid systems are proposed and researched [21, 22]. Many technological systems, such as flotation plants, transportation management, and electropneumatic clutch [23–25], showing typical hybrid dynamic characteristics, can be accurately modeled and controlled by using hybrid systems theory. Several types of models also have been proposed to describe hybrid systems, among which the mixed logical dynamical (MLD) form is capable of modeling the physical laws, logical rules, and operating constraints of hybrid systems through a linear state-space representation [26]. In addition, the hybrid control problem of those dynamical systems modeled by the MLD framework can easily be recast as a mixed-integer linear/quadratic programming problem, which can be solved by existing solvers [27]. Therefore, to design an effective damping multimode switching control strategy for the semiactive axle suspension proposed for the wheel loader, whose damping control process exhibits typical hybrid characteristics, the MLD modeling approach is chosen in this work. Then, to derive the optimal switching sequences of the discrete damping modes by taking the axle suspension performance indices into account, the system damping control problem is further solved by the hybrid MPC strategy. The main contributions of this paper are to apply a new semiactive axle suspension with multiple damping modes for vibration reduction in a wheel loader and to show how the hybrid systems theory can be effectively used to solve both the missions of modeling and optimal control of the proposed semiactive axle suspension.

The rest of this paper is organized as follows. The whole system is described in Section 2, with particular emphasis on the semiactive axle suspension with four discrete damping modes. In Section 3, the system model is derived by using the MLD framework for the wheel loader. Section 4 shows how the system damping multimode switching control problem can be recast as a hybrid MPC scheme. In Section 5, the effectiveness of the proposed semiactive axle suspension and its control method is verified through simulation results. Section 6 ends the paper with some conclusive remarks.

2. System Description

Although most of the wheel loaders are manufactured without any axle suspensions, severe vibration and poor stability are experienced when working under off-road conditions. Therefore, in this study, to improve the ride comfort and driving stability, a wheel loader with axle suspensions is proposed and researched. As shown in Figure 1 [8], the suspensions are installed on the front and rear axles and the front axle to the front body and the rear axle to the rear body are linked, respectively. The vibration transmitted from the tyre to the axle is isolated at a certain degree by the axle suspension firstly and then is transmitted to the driving cab.

The general layout of the target shock absorber with multiple damping modes proposed for the semiactive axle suspension system in a wheel loader can be seen in Figure 2. It is obvious from the figure that the shock absorber is designed based on a conventional monotube hydraulic shock absorber, which mainly consists of a piston assembly (piston road and piston), a rebound chamber, a compression chamber, an air chamber, two valves (rebound and compression valves), and a floating piston. The up and down motions of the piston make the oil pressures of the three chambers change, and thus the hydraulic oil is drove to flow between these different chambers through the hydraulic valves. As shown in Figure 2, the four discrete damping modes are achieved by using the four one-way valves with different oil flow pressure losses and two high-speed switch electromagnetic valves. It is obvious that, by just changing the discrete statuses of the two high-speed switch electromagnetic valves, the hydraulic oil flow path is changed, and thus, the four discrete damping modes can be achieved [28].

According to the aforementioned damping regulation mechanism of the shock absorber, the four damping modes are given in Table 1, in which the discrete statuses of the two high-speed switch electromagnetic valves and the damping characteristics of the four modes are, respectively, provided. Furthermore, the oil flow paths of the four discrete damping modes are shown in Figure 3 [28]. Just as mentioned before, because the oil flow pressure losses of the four one-way valves are different, the different damping characteristics in

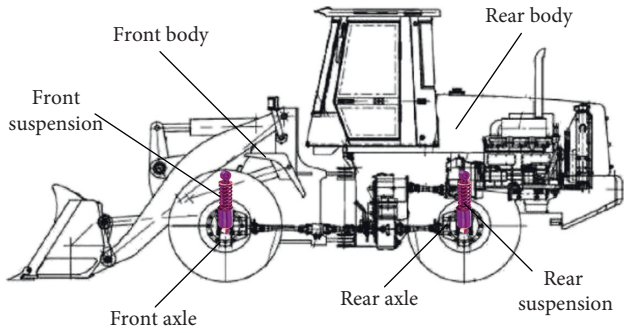

Figure 1: Structure of the wheel loader with axle suspension.

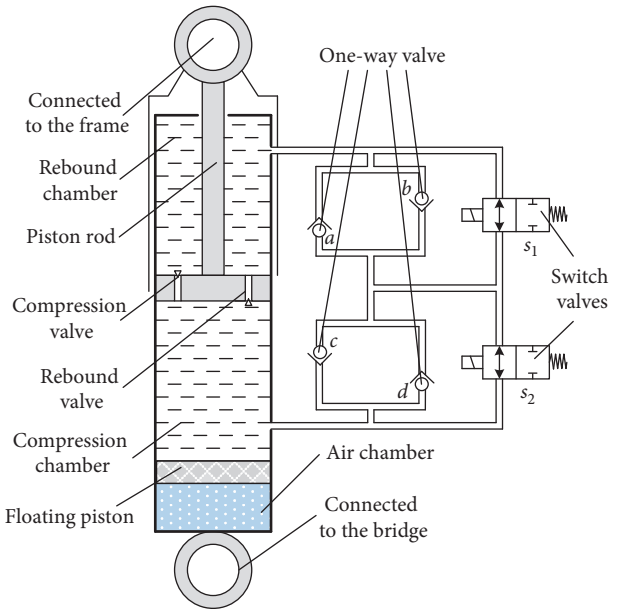

Figure 2: Structure of the shock absorber with multiple damping modes.

Table 1: Four damping modes of the shock absorber.

Damping mode	On-off statuses		Damping characteristics	
	s_1	s_2	Compression stroke	Rebound stroke
1	On	On	Soft	Soft
2	Off	On	Soft	Hard
3	On	Off	Hard	Soft
4	Off	Off	Hard	Hard

the compression and rebound strokes for the four damping modes are also achieved. Concretely speaking, in this work, the oil flow pressure loss of the one-way valve *a* is larger than that of the one-way valve *b*, while oil flow pressure loss of the one-way valve *c* is smaller than that of the one-way valve *b*.

3. System Modeling

In this section, to obtain the optimal switching sequences of the discrete damping modes by considering the vibration isolation requirements, the mathematical model which can accurately describe the system hybrid dynamic characteristics is established. Because the mechanism modeling of the conventional hydraulic shock absorber has been reported in many relevant literatures [29–32], thus in this work, the mathematical modeling of the shock absorber with multiple damping modes is not considered as the introduction emphasis. According to the research results reported in reference [28], the damping force generated by the target shock absorber with multiple damping modes can be represented by the following equations:

$$\begin{cases} F_r = P_r\left(A_p - A_r\right) - P_c A_p = \Delta P_{rc}\left(A_p - A_r\right) - P_c A_r, \\ F_c = P_c A_p - P_r\left(A_p - A_r\right) = \Delta P_{cr}\left(A_p - A_r\right) + P_c A_r, \end{cases} \tag{1}$$

where F_r and F_c are the damping forces of the shock absorber generated in the rebound stroke and the compression stroke, respectively, the oil pressure in the rebound chamber is denoted as P_r, the oil pressure in the compression chamber is denoted as P_c, A_p is the area of piston in the compression chamber, A_r is the area of piston in the rebound chamber, ΔP_{rc} is the differential oil pressure between the rebound chamber and the compression chamber for the rebound stroke, and ΔP_{cr} is the differential oil pressure between the rebound chamber and the compression chamber for the compression stroke. For different damping modes, the values of the variables P_c, ΔP_{rc}, and ΔP_{cr} in Equation (1) are different and influenced by the oil flow paths, thus the different damping characteristics can be achieved. By establishing the mathematical model of the shock absorber with multiple damping modes and calculating the modeling results, the damping coefficients of the target shock absorber in four discrete damping modes are approximately given in Table 2.

Since the multimode switching damping characteristics of the target shock absorber have been linearized approximately, the system hybrid dynamical model can then be established by using the MLD approach. Figure 4 shows a simplified model of the wheel loader semiactive axle suspension with the target shock absorber.

In Figure 4, the parameters characterizing the model include the unsprung mass m_u, the road roughness displacement q_r, the stiffness coefficient of the tyre k_t, the spring stiffness of the axle semiactive suspension k_s, the eight different damping coefficients of the shock absorber with multiple damping modes $c_s(t)$, among of which the damping coefficients of damping mode 1 are denoted as c_{s1-r} and c_{s1-c} for the rebound stroke and the compression stroke respectively, and so on; the damping coefficients for the other three damping modes for the rebound stroke and the compression stroke are denoted as c_{s2-r}, c_{s2-c}, c_{s3-r}, c_{s3-c}, c_{s4-r}, and c_{s4-c}, respectively; the vertical displacement of the unsprung mass by z_u; the vertical displacement and mass of the cab by z_c and m_c; the stiffness and damping coefficients of the seat by k_a and c_a; the vertical displacement and mass of the driver by z_d and m_d; the stiffness and damping coefficients of the power assembly suspension by k_e and c_e; and the vertical displacement and mass of the power assembly by z_e and m_e.

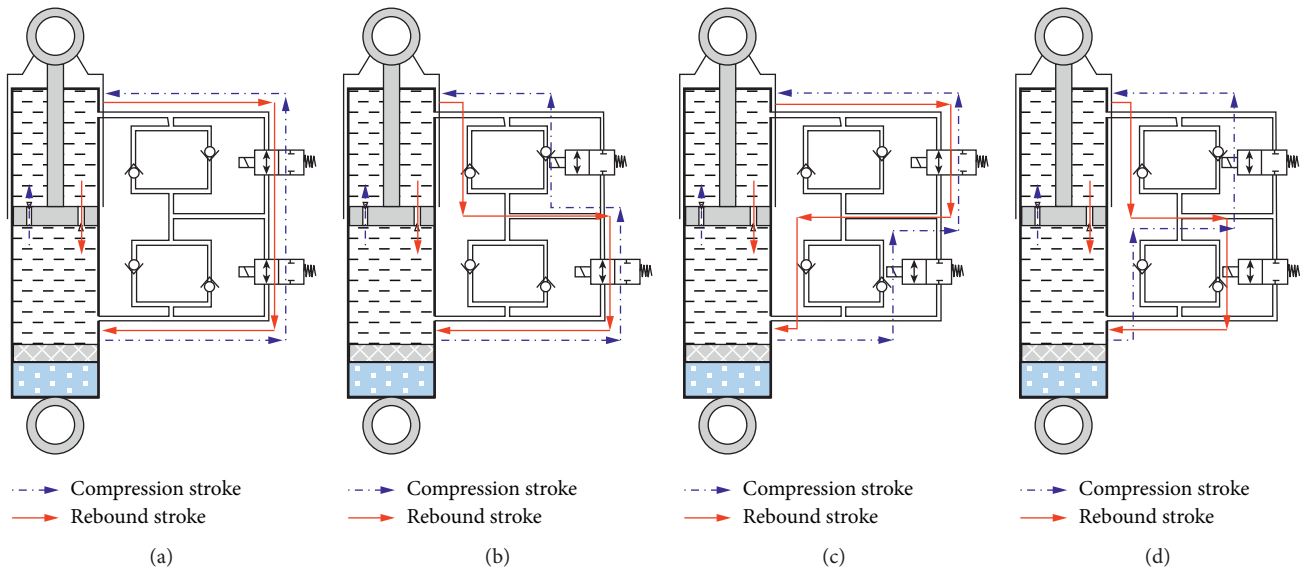

Figure 3: Oil flow paths of the four discrete damping modes (a) 1, (b) 2, (c) 3, and (d) 4.

Table 2: Damping coefficients in different damping modes.

Damping mode		Mode 1	Mode 2	Mode 3	Mode 4
Damping coefficient	Rebound stroke	2112 N·s·m^{-1}	2992 N·s·m^{-1}	2393 N·s·m^{-1}	3590 N·s·m^{-1}
	Compression stroke	968 N·s·m^{-1}	1047 N·s·m^{-1}	1272 N·s·m^{-1}	1483 N·s·m^{-1}

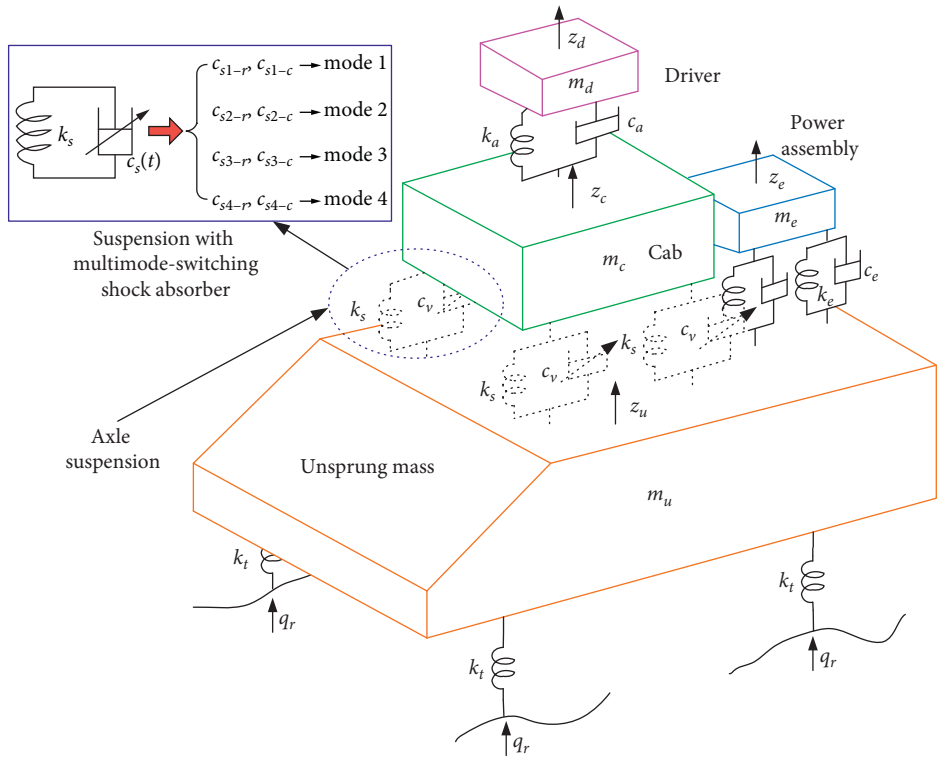

Figure 4: Vibration model of the wheel loader with the target shock absorber.

Because the main research objective of this paper is to design a semiactive suspension control system for vertical vibration reduction in a wheel loader, only the vertical motion is considered, i.e., the roll and pitch motions of the unsprung mass, cab, power assembly, and driver are ignored. Then, the equations of motion of the wheel loader-road vibration system can be given by

$$\begin{cases} m_{\mathrm{u}}\ddot{z}_{\mathrm{u}} = 4k_{\mathrm{t}}(q_{\mathrm{r}} - z_{\mathrm{u}}) - 4k_{\mathrm{s}}(z_{\mathrm{u}} - z_{\mathrm{c}}) - 4c_{\mathrm{s}}(t)(\dot{z}_{\mathrm{u}} - \dot{z}_{\mathrm{c}}) \\ \qquad\qquad - 4k_{\mathrm{e}}(z_{\mathrm{u}} - z_{\mathrm{e}}) - 4c_{\mathrm{e}}(\dot{z}_{\mathrm{u}} - \dot{z}_{\mathrm{e}}), \\ m_{\mathrm{c}}\ddot{z}_{\mathrm{c}} = 4k_{\mathrm{s}}(z_{\mathrm{u}} - z_{\mathrm{c}}) + 4c_{\mathrm{s}}(t)(\dot{z}_{\mathrm{u}} - \dot{z}_{\mathrm{c}}) - k_{\mathrm{a}}(z_{\mathrm{c}} - z_{\mathrm{d}}) \\ \qquad\qquad - c_{\mathrm{a}}(\dot{z}_{\mathrm{c}} - \dot{z}_{\mathrm{d}}), \\ m_{\mathrm{e}}\ddot{z}_{\mathrm{e}} = 4k_{\mathrm{e}}(z_{\mathrm{u}} - z_{\mathrm{e}}) + 4c_{\mathrm{e}}(\dot{z}_{\mathrm{u}} - \dot{z}_{\mathrm{e}}), \\ m_{\mathrm{d}}\ddot{z}_{\mathrm{d}} = k_{\mathrm{a}}(z_{\mathrm{c}} - z_{\mathrm{d}}) + c_{\mathrm{a}}(\dot{z}_{\mathrm{c}} - \dot{z}_{\mathrm{d}}). \end{cases} \tag{2}$$

As mentioned before, the damping mode of the target shock absorber depends on the discrete statuses of the two high-speed switch electromagnetic valves; thus to obtain the optimal switching sequences of the discrete damping modes for the wheel loader semiactive axle suspension, the system hybrid model should be further established based on Equation (2). According to the description of the MLD framework [33], the general model form of the damping hybrid control process is given by

$$\begin{cases} \mathbf{x}(t+1) = \mathbf{A}\mathbf{x}(t) + \mathbf{B_1}\mathbf{u}(t) + \mathbf{B_2}\boldsymbol{\delta}(t) + \mathbf{B_3}\mathbf{z}(t), \\ \mathbf{y}(t) = \mathbf{C}\mathbf{x}(t) + \mathbf{D_1}\mathbf{u}(t) + \mathbf{D_2}\boldsymbol{\delta}(t) + \mathbf{D_3}\mathbf{z}(t), \\ \mathbf{E_2}\boldsymbol{\delta}(t) + \mathbf{E_3}\mathbf{z}(t) \le \mathbf{E_1}\mathbf{u}(t) + \mathbf{E_4}\mathbf{x}(t) + \mathbf{E_5}, \end{cases} \tag{3}$$

where $\mathbf{x}(t) \in \Re^{n_{\mathrm{c}}} \times \{0,1\}^{n_{\mathrm{l}}}$, $\mathbf{u}(t) \in \Re^{m_{\mathrm{c}}} \times \{0,1\}^{m_{\mathrm{l}}}$, and $\mathbf{y}(t) \in \Re^{r_{\mathrm{c}}} \times \{0,1\}^{r_{\mathrm{l}}}$ denote the system state, input vector, and output vector, respectively. Additionally, $\boldsymbol{\delta}(t) \in \{0,1\}^{p_{\mathrm{l}}}$ and $\mathbf{z}(t) \in \Re^{p_{\mathrm{c}}}$ are the auxiliary binary and continuous variables, respectively. The evolutions of the state variables are described by the state matrix $\mathbf{A}$ and the input matrices $\mathbf{B}_1$, $\mathbf{B}_2$, and $\mathbf{B}_3$. Similarly, the evolutions of the output variables are described by the output matrix $\mathbf{C}$ and the matrices $\mathbf{D}_1$, $\mathbf{D}_2$, and $\mathbf{D}_3$. Finally, the system inequalities are defined by the matrices $\mathbf{E}_1$ to $\mathbf{E}_5$. The MLD system is useful to describe several types of hybrid systems and is also able to recast hybrid system dynamic control problems into mixed-integer linear or quadratic programs solvable via efficient solvers. This feature has led this system to be widely used in the formulation of hybrid control strategies [34].

For complex dynamics systems, the establishment of the MLD model is inefficient and tedious if using traditional methods; thus a language called HYSDEL, which can generate the standard form of the MLD model defined by Equation (3) automatically, is developed by Torrisi and Bemporad [35]. According to the compile process of HYSDEL, how the damping multimode switching control process of the wheel loader semiactive axle suspension can be modeled as a MLD system is then introduced.

The first step is the definition of the system-state variables, which are defined as follows:

$$\mathbf{x} = [z_u \; z_c \; z_e \; z_d \; \dot{z}_u \; \dot{z}_c \; \dot{z}_e \; \dot{z}_d]. \tag{4}$$

To achieve the direct control of the discrete statuses of the two high-speed switch electromagnetic valves, which also determine the damping mode switching sequences, the system control variables are defined as

$$\mathbf{u} = [\delta_1 \; \delta_2 \; q_{\mathrm{r}}], \tag{5}$$

where δ_1 denotes the discrete status of the high-speed switch electromagnetic valve S_1 and δ_2 denotes the discrete status of the high-speed switch electromagnetic valve S_2. By considering the vibration isolation performance requirements, the system output variables are defined as

$$\mathbf{y} = [\ddot{z}_{\mathrm{d}} \; z_{\mathrm{u}} \; -z_{\mathrm{c}}]. \tag{6}$$

Meanwhile, the parameters of the vibration model of the wheel loader with a semiactive axle suspension, which will be used in the following simulation analyses, are listed in Table 3.

Furthermore, the relationship between the two logical input variables and the discrete statuses of the high-speed switch electromagnetic valves are defined as [28]

$$\begin{aligned} [\delta_1 = 1] &\longleftrightarrow S_1 \text{ is open}, \\ [\delta_2 = 1] &\longleftrightarrow S_2 \text{ is open}. \end{aligned} \tag{7}$$

On this basis, the following four auxiliary variables are defined to represent the four damping modes:

$$\begin{cases} [\delta_{\mathrm{m1}} = 1] \longleftrightarrow \text{mode 1}, \\ [\delta_{\mathrm{m2}} = 1] \longleftrightarrow \text{mode 2}, \\ [\delta_{\mathrm{m3}} = 1] \longleftrightarrow \text{mode 3}, \\ [\delta_{\mathrm{m4}} = 1] \longleftrightarrow \text{mode 4}. \end{cases} \tag{8}$$

It is obvious that these four auxiliary variables have the following relationships with δ_1 and δ_2:

$$\begin{cases} \delta_{\mathrm{m1}} = \delta_1 \wedge \delta_2, \\ \delta_{\mathrm{m2}} = \overline{\delta}_1 \wedge \delta_2, \\ \delta_{\mathrm{m3}} = \delta_1 \wedge \overline{\delta}_2, \\ \delta_{\mathrm{m4}} = \overline{\delta}_1 \wedge \overline{\delta}_2. \end{cases} \tag{9}$$

Because the shock absorber damping characteristics are influenced by the piston strokes, two auxiliary logical variables are further defined to reflect the rebound stroke and the compression stroke, respectively:

$$\begin{aligned} [\delta_{\mathrm{su}} = 1] &\longleftrightarrow \dot{z}_{\mathrm{s}} - \dot{z}_{\mathrm{u}} > 0, \\ [\delta_{\mathrm{su}} = 0] &\longleftrightarrow \dot{z}_{\mathrm{s}} - \dot{z}_{\mathrm{u}} < 0. \end{aligned} \tag{10}$$

Hence, the damping coefficient of the shock absorber with multiple damping modes can be expressed as

$$\begin{aligned} c_{\mathrm{s}}(t) = {} & \delta_{\mathrm{c1-r}}c_{\mathrm{s1-r}} + \delta_{\mathrm{c1-c}}c_{\mathrm{s1-c}} + \delta_{\mathrm{c2-r}}c_{\mathrm{s2-r}} + \delta_{\mathrm{c2-c}}c_{\mathrm{s2-c}} \\ & + \delta_{\mathrm{c3-r}}c_{\mathrm{s3-r}} + \delta_{\mathrm{c3-c}}c_{\mathrm{s3-c}} + \delta_{\mathrm{c4-r}}c_{\mathrm{s4-r}} + \delta_{\mathrm{c4-c}}c_{\mathrm{s4-c}}. \end{aligned} \tag{11}$$

The auxiliary logical variables $\delta_{\mathrm{c1-r}}$, $\delta_{\mathrm{c1-c}}$, $\delta_{\mathrm{c2-r}}$, $\delta_{\mathrm{c2-c}}$, $\delta_{\mathrm{c3-r}}$, $\delta_{\mathrm{c3-c}}$, $\delta_{\mathrm{c4-r}}$, and $\delta_{\mathrm{c4-c}}$ are defined as

Table 3: Parameter values of the vibration model of the wheel loader.

Parameter	Value	Parameter	Value
m_u	15915 kg	m_e	450 kg
k_t	392000 N·m^{-1}	m_c	235 kg
k_s	49500 N·m^{-1}	k_a	25000 N·m^{-1}
k_e	16000 N·m^{-1}	c_a	1835 N·s·m^{-1}
c_e	2108 N·s·m^{-1}	m_d	75 kg

$$\begin{cases} \delta_{c1-r} = \delta_{su} \wedge \delta_{m1}, \\ \delta_{c1-c} = \overline{\delta}_{su} \wedge \delta_{m1}, \\ \delta_{c2-r} = \delta_{su} \wedge \delta_{m2}, \\ \delta_{c2-c} = \overline{\delta}_{su} \wedge \delta_{m2}, \\ \delta_{c3-r} = \delta_{su} \wedge \delta_{m3}, \\ \delta_{c3-c} = \overline{\delta}_{su} \wedge \delta_{m3}, \\ \delta_{c4-r} = \delta_{su} \wedge \delta_{m4}, \\ \delta_{c4-c} = \overline{\delta}_{su} \wedge \delta_{m4}. \end{cases} \tag{12}$$

Based on Equations (11) and (12), the following eight auxiliary continuous variables are defined as

$$\begin{cases} z_{c1-r} = \delta_{c1-r} c_{s1-r}, \\ z_{c1-c} = \delta_{c1-c} c_{s1-c}, \\ z_{c2-r} = \delta_{c2-r} c_{s2-r}, \\ z_{c2-c} = \delta_{c2-c} c_{s2-c}, \\ z_{c3-r} = \delta_{c3-r} c_{s3-r}, \\ z_{c3-c} = \delta_{c3-c} c_{s3-c}, \\ z_{c4-r} = \delta_{c4-r} c_{s4-r}, \\ z_{c4-c} = \delta_{c4-c} c_{s4-c}. \end{cases} \tag{13}$$

Thus, the variable damping coefficients of the target shock absorber can be further expressed as

$$\begin{aligned} c_s(t) = {} & z_{c1-r} + z_{c1-c} + z_{c2-r} + z_{c2-c} + z_{c3-r} \\ & + z_{c3-c} + z_{c4-r} + z_{c4-c}. \end{aligned} \tag{14}$$

Furthermore, due to the discrete-time characteristics of the MLD framework, the discretization of the system state variables is further carried out as follows:

$$\begin{cases} \ddot{z}_u = \dfrac{(\dot{z}_u(t+1) - \dot{z}_u(t))}{T_s}, \\ \ddot{z}_c = \dfrac{(\dot{z}_c(t+1) - \dot{z}_c(t))}{T_s}, \\ \ddot{z}_e = \dfrac{(\dot{z}_e(t+1) - \dot{z}_e(t))}{T_s}, \\ \ddot{z}_d = \dfrac{(\dot{z}_d(t+1) - \dot{z}_d(t))}{T_s}, \\ \dot{z}_u = \dfrac{(z_u(t+1) - z_u(t))}{T_s}, \\ \dot{z}_c = \dfrac{(z_c(t+1) - z_c(t))}{T_s}, \\ \dot{z}_e = \dfrac{(z_e(t+1) - z_e(t))}{T_s}, \\ \dot{z}_d = \dfrac{(z_d(t+1) - z_d(t))}{T_s}, \end{cases} \tag{15}$$

where T_s is the sampling time. Then, based on the dynamics equations shown in Eq. (2), the linear update equations for system-state variables, which are important for the system MLD modeling, can be given by

$$\begin{cases} z_u(t+1) = z_u(t) + T_s \dot{z}_u(t), z_c(t+1) = z_c(t) + T_s \dot{z}_c(t), \\ z_e(t+1) = z_e(t) + T_s \dot{z}_e(t), z_d(t+1) = z_d(t) + T_s \dot{z}_d(t), \\ \dot{z}_u(t+1) = \dot{z}_u(t) + \dfrac{4T_s k_t}{m_u}(q_r(t) - z_u(t)) - \dfrac{4T_s k_s}{m_u}(z_u(t) - z_c(t)), \\ - \dfrac{4T_s[z_{c1-r} + z_{c1-c} + z_{c2-r} + z_{c2-c} + z_{c3-r} + z_{c3-c} + z_{c4-r} + z_{c4-c}]}{m_u}(\dot{z}_u(t) - \dot{z}_c(t)) - \dfrac{4T_s k_e}{m_u}(z_u(t) - z_e(t)) - \dfrac{4T_s c_e}{m_u}(\dot{z}_u(t) - \dot{z}_e(t)), \\ \dot{z}_c(t+1) = \dot{z}_c(t) + \dfrac{4T_s k_s}{m_c}(z_u(t) - z_c(t)) + \dfrac{4T_s[z_{c1-r} + z_{c1-c} + z_{c2-r} + z_{c2-c} + z_{c3-r} + z_{c3-c} + z_{c4-r} + z_{c4-c}]}{m_c}(\dot{z}_u(t) - \dot{z}_c(t)), \\ - \dfrac{T_s k_a}{m_c}(z_c(t) - z_d(t)) - \dfrac{4T_s c_a}{m_c}(\dot{z}_c(t) - \dot{z}_d(t)), \\ \dot{z}_e(t+1) = \dot{z}_e(t) + \dfrac{4T_s k_e}{m_e}(z_u(t) - z_e(t)) + \dfrac{4T_s c_e}{m_e}(\dot{z}_u(t) - \dot{z}_e(t)), \\ \dot{z}_d(t+1) = \dot{z}_d(t) + \dfrac{4T_s k_a}{m_d}(z_c(t) - z_d(t)) + \dfrac{4T_s c_a}{m_d}(\dot{z}_c(t) - \dot{z}_d(t)). \end{cases} \tag{16}$$

To help in solving the mixed-integer programming problem, which will be used in the hybrid MPC strategy design, the following constraints on the defined logical variables can be further introduced based on the system actual working process:

$$\begin{cases} \delta_{m1} + \delta_{m2} + \delta_{m3} + \delta_{m4} \le 1, \\ \delta_{c1-r} + \delta_{c1-c} + \delta_{c2-r} + \delta_{c2-c} + \delta_{c3-r} + \delta_{c3-c} \\ \quad + \delta_{c4-r} + \delta_{c4-c} \le 1. \end{cases} \tag{17}$$

Through the above modeling process by using HYSDEL, the standard form of the system MLD model of the wheel loader semiactive axle suspension, which contains the target shock absorber with multiple damping modes, can then be established automatically by compiling the HYSDEL process. In this work, the HYSDEL version 3.0 is applied to establish the system MLD model, and a Simulink module named as "HYSDEL model" can be obtained finally [36]. Since the paper space is limited, the specific forms of the 68 MLD inequalities are omitted here.

4. Adaptive Control Strategy

In this section, to achieve the optimal control of the target shock absorber with multiple damping modes for the wheel loader semiactive axle suspension by considering the vibration isolation requirements, a hybrid MPC approach is applied. The hybrid MPC strategy uses the established MLD model as the prediction model and solves a constrained optimal control problem at each sampling instant over a finite horizon using the current state as the initial state. Then, an optimal control sequence, which can minimize a given objective function, is got. In particular, the receding horizon policy of the hybrid MPC strategy is achieved by only applying the first control input in the sequence and by recomputing the control sequence at the next sampling instant, which makes it have good adaptability [37, 38].

In order to improve the vibration reduction performance of the wheel loader, the decrease of the vertical acceleration of the driver is the system primary control objective. However, it is obvious that although the soft suspension can reduce the system vibration, too soft suspension will increase the suspension deflection; thus the probability of suspension reaching the mechanical end stop increases. Therefore, the suspension deflection, $z_u - z_c$, needs to be limited during the controller design process. In addition, to guarantee the system stability and the operating lifespan of the high-speed switch electromagnetic valves, the frequent switching of the discrete statuses of the switch electromagnetic valves should also be prevented, which can be achieved by minimizing the number of switch transitions within the prediction interval. Consequently, the system objective function accounting for optimal control of the damping characteristics and adherence to the vibration isolation requirements is defined as follows:

$$J = \sum_{h=0}^{N-1} \|\mathbf{y}(h \mid t)\|_{\mathbf{Q}_y}^2 + \|\Delta \mathbf{u}(h \mid t)\|_{\mathbf{Q}_u}^2, \tag{18}$$

where $\mathbf{Q}_y = \mathrm{diag}\,(q_r, q_d)$ is the penalty weighting matrix for the system outputs and $\mathbf{Q}_u = \mathrm{diag}\,(r_{\delta 1}, r_{\delta 2})$ is the penalty matrix for the difference between four consecutive control inputs, which is defined as

$$\begin{aligned} \Delta \mathbf{u}(t) &= \left[\Delta\delta_1(t) \Delta\delta_2(t)\right]^T \\ &= \left[\delta_1(t) - \delta_1(t-1) \delta_2(t) - \delta_2(t-1)\right]^T. \end{aligned} \tag{19}$$

On the basis of the established MLD model (3) and the defined objective function (18), the system optimal control inputs, i.e., the switching sequences of the damping modes, at time instant t can then be calculated by minimizing the defined objective function over the sequence of control inputs subject to the mixed-integer inequality constraints. Then, a constrained finite time optimal problem can be obtained as [39]

$$\begin{aligned} \min_{\mathbf{U}_N(t)} \quad & \sum_{h=0}^{N-1} \|\mathbf{y}(h \mid t)\|_{\mathbf{Q}_y}^2 + \|\Delta \mathbf{u}(h \mid t)\|_{\mathbf{Q}_u}^2, \\ \text{s.t.} \quad & \mathbf{x}(0 \mid t) = \mathbf{x}(t), \\ & \mathbf{x}(t+1) = \mathbf{A}\mathbf{x}(t) + \mathbf{B}_1\mathbf{u}(t) + \mathbf{B}_2\boldsymbol{\delta}(t) + \mathbf{B}_3\mathbf{z}(t), \\ & \mathbf{y}(t) = \mathbf{C}\mathbf{x}(t) + \mathbf{D}_1\mathbf{u}(t) + \mathbf{D}_2\boldsymbol{\delta}(t) + \mathbf{D}_3\mathbf{z}(t), \\ & \mathbf{E}_2\boldsymbol{\delta}(t) + \mathbf{E}_3\mathbf{z}(t) \le \mathbf{E}_1\mathbf{u}(t) + \mathbf{E}_4\mathbf{x}(t) + \mathbf{E}_5, \\ & \mathbf{u}_{\min} \le \mathbf{u}(h \mid t) \le \mathbf{u}_{\max}, \\ & \mathbf{x}_{\min} \le \mathbf{x}(h \mid t) \le \mathbf{x}_{\max}, \end{aligned} \tag{20}$$

whose solution is the optimal system control sequence, of which only the first element $\boldsymbol{U}_N(t)$ is applied to the system at time instant t. After the system states and outputs are newly estimated/measured at the next time instant, the aforementioned optimal control procedure is then repeated. Because the defined objective function (18) uses the 2 norm, the optimal problem (20) can then be regarded as a mixed-integer quadratic program (MIQP) problem [40].

By setting the following three vectors

$$\begin{cases} \boldsymbol{\Omega} = \left[\mathbf{u}^T(0 \mid t) \cdots \mathbf{u}^T(N-1 \mid t)\right]^T, \\ \boldsymbol{\Xi} = \left[\boldsymbol{\delta}^T(0 \mid t) \cdots \boldsymbol{\delta}^T(N-1 \mid t)\right]^T, \\ \Gamma = \left[\mathbf{z}^T(0 \mid t) \cdots \mathbf{z}^T(N-1 \mid t)\right]^T, \end{cases} \tag{21}$$

and the general vector

$$\boldsymbol{\Lambda} = \left[\boldsymbol{\Omega}^T \boldsymbol{\Xi}^T \Gamma^T\right]^T, \tag{22}$$

the MIQP problem of the wheel loader semiactive axle suspension, which contains the target shock absorber with multiple damping modes, can then be solved as follows:

$$\begin{aligned} \min_{\{\boldsymbol{\Lambda}\}} \quad & \frac{1}{2}\boldsymbol{\Lambda}^T \mathbf{S}_1 \boldsymbol{\Lambda} + \mathbf{S}_2 \boldsymbol{\Lambda}, \\ \text{Subj.to.} \quad & \mathbf{S}_3 \boldsymbol{\Lambda} \le \mathbf{S}_4, \end{aligned} \tag{23}$$

where $\mathbf{S}_1$, $\mathbf{S}_2$, $\mathbf{S}_3$, and $\mathbf{S}_4$ are matrices with suitable dimensions. Considering the characteristics of the research problem in this study, the branch and bound method is used to solve the MIQP problem [41]. The main idea of the branch and bound method for solving the MIQP problem is to lift

partial or whole integer restrictions in the decision variables; thus a series of quadratic programming (QP) problems which follow the original MIQP problem are formed. Since the solution of the QP problem is relatively simple, the suboptimal solution or global optimal solution of the MIQP problem which meets the integer constraints can be obtained by solving a series of QP problems. Although the MIQP problem has exponential complexity, efficient numerical solvers for its solution are available, e.g., CPLEX.

5. Simulation Study

To verify the vibration reduction performance of the proposed semiactive axle suspension with multiple damping modes for the wheel loader and the effectiveness of its hybrid MPC approach, numerical simulation results are presented in this section. To reflect the major disturbances acting on the wheel loader semiactive axle suspensions, the bump road and the random road irregularity excitations are chosen to model the real-world road roughness disturbances.

5.1. Simulation Analysis of the First Case. The first road irregularity excitation is a single bump input, which is often used to reflect the transient response characteristics of the wheel loader axle suspension. Considering the case of a bump input on a smooth road surface, the road displacement input in time domain can be given by [42]

$$q_{\mathrm{r}}(t) = \begin{cases} \dfrac{A_{\mathrm{m}}}{2}\left(1 - \cos\dfrac{2\pi v}{L}t\right), & 0 \le t \le \dfrac{L}{v}, \\ 0, & t > \dfrac{L}{v}, \end{cases} \tag{24}$$

where A_{m} denotes the bump height, L denotes the bump length and v denotes the wheel loader forward velocity. During the simulation calculation process, A_{m} and L are, respectively, set to 0.2 m and 0.45 m and the wheel loader forward velocity is set to 0.6 m/s. By applying the bump road excitation input to the wheel loader axle suspension, the transient responses of the passive system with a conventional shock absorber (denoted as Passive), the conventional wheel loader semiactive axle suspension controlled by a PID controller (denoted as PID), and the wheel loader semiactive axle suspension, which contains the target shock absorber with multiple damping modes, controlled by the hybrid MPC methodology (denoted as HMPC) are compared in Figures 5 and 6.

It can be seen from Figures 5 and 6 that significant improvement of the vibration isolation performance is achieved for the wheel loader semiactive axle suspension controlled by HMPC compared with the passive suspension and the conventional semiactive suspension controlled by PID. As shown in Figure 5, the peak value of the driver vertical acceleration can be reduced significantly by both proposed wheel loader semiactive axle suspension controlled by HMPC and conventional wheel loader semiactive axle suspension controlled by a PID controller. However, the time needed to reach a stable value for the former is shorter and the rate of reduction is even larger, which demonstrates the potential advantages of the proposed wheel loader semiactive axle suspension, which contains the target shock absorber with multiple damping modes, controlled by using the hybrid MPC methodology. The same simulation results for the suspension deflection under bump input can also be obtained from Figure 6, which verifies that the system control objectives reflected in the objective function are achieved effectively by the designed control strategy.

5.2. Simulation Analysis of the Second Case. The second type of the road irregularity excitation is the random road input, which also represents the disturbances that often act on the wheel loader axle suspension. By using the rational function, the time domain representation of the random road input can be given by [43, 44]

$$\dot{q}_{\mathrm{r}}(t) = -0.111\left[v q_{\mathrm{r}}(t) + 40\sqrt{G_{\mathrm{q}}(n_0)v}\, w(t)\right], \tag{25}$$

where $G_{\mathrm{q}}(n_0)$ denotes the road roughness coefficient and $w(t)$ is the Gaussian white noise with zero mean value. To conduct the simulation calculation, the wheel loader is assumed to be driven on a rough road corresponding to the class D of ISO road profiles at 20 km/h. Similarly, in this case, the time responses of the wheel loader passive suspension, the conventional semiactive axle suspension controlled by a PID controller and the proposed axle suspension, which contains the target shock absorber with multiple damping modes, controlled by HMPC are compared. Figures 7 and 8 show the comparison results. Moreover, to better show the effectiveness of the proposed semiactive axle suspension for the wheel loader and its control approach, the RMS values of the suspension performance indices are also listed in Table 4.

As shown in Figures 7, 8 and Table 4, similar conclusions can be summarized for this case where the proposed semiactive suspension and its control method are effective in improving the wheel loader vibration isolation performance. In particular, the wheel loader semiactive axle suspension, which contains the target shock absorber with multiple damping modes, controlled by HMPC can reduce the RMS values of the driver vertical acceleration and the suspension deflection by 42.36% and 60.37%, respectively, compared with the conventional passive suspension. These improvements are even larger than that of the traditional semiactive suspension with continuously adjustable shock absorber controlled by PID, whose RMS value improvements of the driver vertical acceleration and the suspension deflection are, 26.22% and 47.17% respectively. The simulation results confirm that better performance of the wheel loader axle suspension can be achieved by the target shock absorber and the proposed HMPC approach.

Figure 9 further shows the discrete status variations of the two high-speed switch electromagnetic valves provided by the HMPC controller. On this basis, the optimal switching sequences of the discrete damping modes can be presented in Figure 10. As shown in these two figures, the designed HMPC controller can achieve an effective control for the discrete statuses of the two high-speed switch

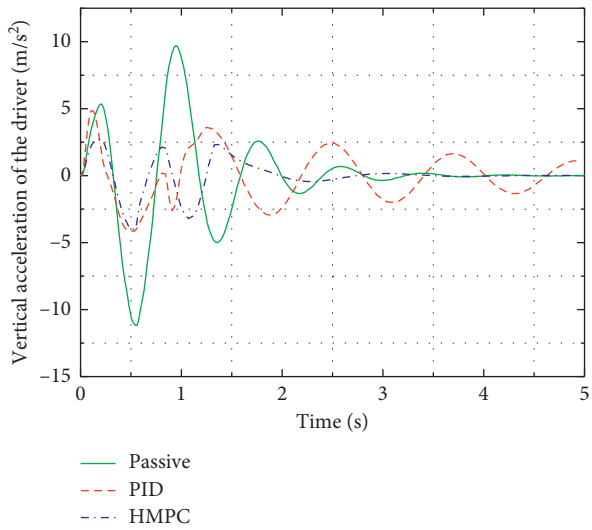

Figure 5: Vertical acceleration of the driver under bump input.

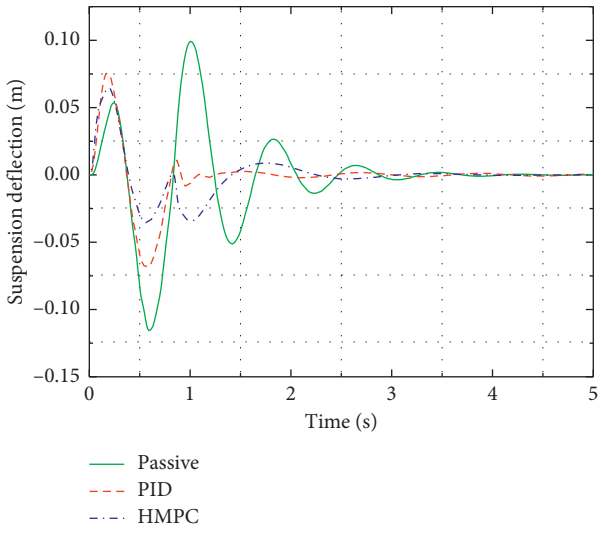

Figure 6: Suspension deflection under bump input.

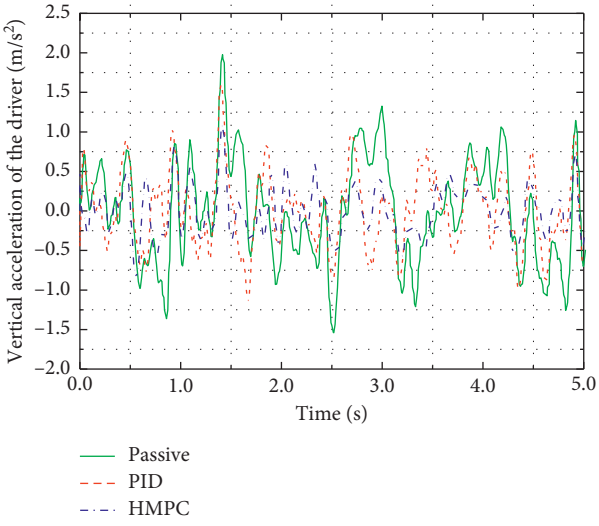

Figure 7: Vertical acceleration of the driver under random input.

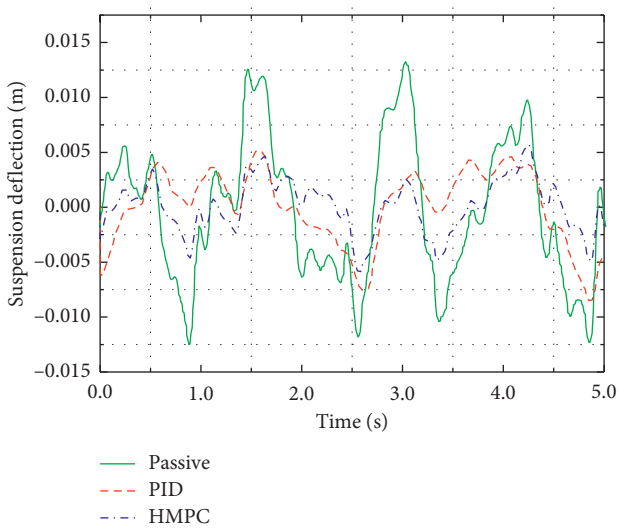

Figure 8: Suspension deflection under random input.

Table 4: RMS value comparison under random road input.

Performance	Passive	PID		HMPC	
	RMS	RMS	Decrease	RMS	Decrease
$\ddot{z}_d$ (m/s^2)	0.713	0.526	26.22%	0.411	42.36%
$z_u - z_c$ (m)	0.0053	0.0028	47.17%	0.0021	60.37%

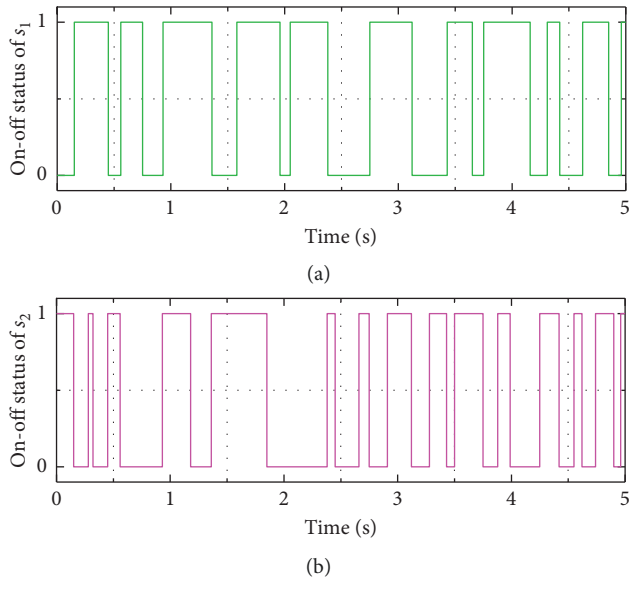

Figure 9: On-off status variations of the solenoid valves.

electromagnetic valves, which demonstrates the effectiveness of the HMPC approach for obtaining the optimal switching sequences of the discrete damping modes by considering the vibration isolation performance requirements. It is also noted that since the proposed wheel loader semiactive axle suspension, which contains the target shock absorber with multiple damping modes, poses challenging hybrid control problem, the hybrid MPC controller designed in this work is the only effective control strategy that we can provide

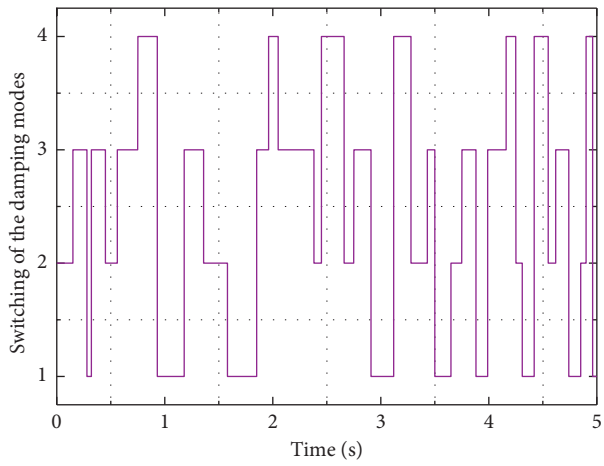

Figure 10: Switching of the damping modes.

currently. In future studies, the comparison between the performances of the hybrid MPC controller with other effective hybrid control strategies is considered to be conducted.

6. Conclusions

In this work, the idea of using semiactive axle suspension for reducing the vibration in a wheel loader has been developed. The system actuators are the damping multimode switching shock absorbers whose damping characteristics are determined by the discrete statuses of two high-speed switch electromagnetic valves. The idea is to adapt online the optimal switching sequences of the four discrete damping modes by using hybrid MPC strategy in order to reduce vibration level transmitted to the wheel loader driver. The system has been analyzed, and the hybrid dynamical model has been established based on the MLD framework. On this basis, a hybrid MPC controller has been tuned, which achieves the optimal control of the discrete damping modes by considering the vibration isolation performance requirements. The performance comparisons between the conventional passive suspension, the conventional semiactive suspension controlled by PID, and the proposed axle suspension, which contains the target shock absorber with multiple damping modes, controlled by HMPC are conducted by numerical simulations. Simulation results verify the effectiveness of the proposed control approach for obtaining the optimal switching sequences of the discrete damping modes and demonstrate the advantages of the proposed axle suspension and its control approach on improving the vibration isolation performance of the wheel loader.

Data Availability

The data used to support the findings of this study are available from the corresponding author upon request.

Conflicts of Interest

The authors declare that they have no conflicts of interest.

Acknowledgments

This work was supported by the National Natural Science Foundation of China (grant no. 51508031) and the Department of Road and Bridge Engineering, Jiangsu Jiaotong College.

References

[1] L. Evers, F. Krause, and P. Vink, "Aspects to improve cabin comfort of wheel loaders and excavators according to operators," *Applied Ergonomics*, vol. 34, no. 3, pp. 265–271, 2003.

[2] R. Fales, E. Spencer, K. Chipperfield et al., "Modeling and control of a wheel loader with a human-in-the-loop assessment using virtual reality," *Journal of Dynamic Systems, Measurement, and Control*, vol. 127, no. 9, pp. 415–423, 2005.

[3] X. Zhao, M. Kremb, and C. Schindler, "Assessment of wheel loader vibration on the riding comfort according to ISO standards," *Vehicle System Dynamics*, vol. 51, no. 10, pp. 1548–1567, 2013.

[4] X. Zhao and C. Schindler, "Evaluation of whole-body vibration exposure experienced by operators of a compact wheel loader according to ISO 2631-1:1997 and ISO 2631-5:2004," *International Journal of Industrial Ergonomics*, vol. 44, no. 6, pp. 840–850, 2014.

[5] F. Chi, J. Zhou, Q. Zhang, Y. Wang, and P. Huang, "Avoiding the health hazard of people from construction vehicles: a strategy for controlling the vibration of a wheel loader," *International Journal of Environmental Research and Public Health*, vol. 14, no. 3, p. 275, 2017.

[6] D. Cao, X. Song, and M. Ahmadian, "Editors' perspectives: road vehicle suspension design, dynamics, and control," *Vehicle System Dynamics*, vol. 49, no. 1-2, pp. 3–28, 2011.

[7] A. Pazooki, *Ride and directional dynamic analysis of articulated frame steer vehicles*, Ph.D. Thesis, Concordia University, Montreal, QC, Canada, 2012.

[8] X. Li, W. Lv, W. Zhang et al., "Research on dynamic behaviors of wheel loaders with different layout of hydropneumatic suspension," *Journal of Vibroengineering*, vol. 19, no. 7, pp. 5388–5404, 2017.

[9] A. Rehnberg and L. Drugge, "Ride comfort simulation of a wheel loader with suspended axles," *International Journal of Vehicle Systems Modelling and Testing*, vol. 3, no. 3, pp. 168–188, 2008.

[10] Y. Sun and Z. Wu, "Dynamic parameter matching schemes of three-axis vehicles suspension," *Journal of Jiangsu University: Natural Science Editions*, vol. 39, no. 4, pp. 249–253, 2018.

[11] K. C. Le and A. Pieper, "Damping of roll vibrations of vehicle suspension," *Vehicle System Dynamics*, vol. 52, no. 4, pp. 562–579, 2014.

[12] N. Yagiz and Y. Hacioglu, "Backstepping control of a vehicle with active suspensions," *Control Engineering Practice*, vol. 16, no. 12, pp. 1457–1467, 2008.

[13] X. Sun, Y. Cai, C. Yuan et al., "Hybrid model predictive control of damping multi-mode switching damper for vehicle suspensions," *Journal of Vibroengineering*, vol. 19, no. 4, pp. 2910–2930, 2017.

[14] I. Youn and A. Hać, "Semi-active suspensions with adaptive capability," *Journal of Sound and Vibration*, vol. 180, no. 3, pp. 475–492, 1995.

[15] H. Zhang, E. Wang, N. Zhang et al., "Semi-active sliding mode control of vehicle suspension with magneto-rheological damper," *Chinese Journal of Mechanical Engineering*, vol. 28, no. 1, pp. 63–75, 2015.

[16] L. Liu, Y. Zhou, Y. Mi et al., "Performance parameter optimization of excavator cab shock absorbers based on Kriging method," *Journal of Jiangsu University: Natural Science Editions*, vol. 36, no. 5, pp. 497–503, 2015.

[17] H. Du, W. Li, and N. Zhang, "Integrated seat and suspension control for a quarter car with driver model," *IEEE Transactions on Vehicular Technology*, vol. 61, no. 9, pp. 3893–3908, 2012.

[18] M. Hoseinzadeh and J. Rezaeepazhand, "Vibration suppression of composite plates using smart electrorheological dampers," *International Journal of Mechanical Sciences*, vol. 84, pp. 31–40, 2014.

[19] Y. Kang, H. Pang, K. Liu, J. Yang, and X. Chai, "Research on skyhook control strategy of multi-grade adjustable damper in semi-active air suspension," *Mechanical Science and Technology for Aerospace Engineering*, vol. 35, no. 5, pp. 778–783, 2016.

[20] L. Chen, L. Yu, and X. Cui, "Performance simulation and testing of multi-levels-damping adjustable hydraulic shock absorber," *Journal of Jiangsu University: Natural Science Editions*, vol. 34, no. 3, pp. 249–253, 2013.

[21] X. Sun, Y. Cai, S. Wang, Y. Liu, and L. Chen, "A hybrid approach to modeling and control of vehicle height for electronically controlled air suspension," *Chinese Journal of Mechanical Engineering*, vol. 29, no. 1, pp. 152–162, 2016.

[22] W. P. M. H. Heemels, B. De Schutter, and A. Bemporad, "Equivalence of hybrid dynamical models," *Automatica*, vol. 37, no. 7, pp. 1085–1091, 2001.

[23] E. Putz and A. Cipriano, "Hybrid model predictive control for flotation plants," *Minerals Engineering*, vol. 70, pp. 26–35, 2015.

[24] I. I. Sirmatel and N. Geroliminis, "Dynamical modeling and predictive control of bus transport systems: a hybrid systems approach," *IFAC-PapersOnLine*, vol. 50, no. 1, pp. 7499–7504, 2017.

[25] B. Szimandl and H. Németh, "Dynamic hybrid model of an electro-pneumatic clutch system," *Mechatronics*, vol. 23, no. 1, pp. 21–36, 2013.

[26] A. Bemporad and M. Morari, "Control of systems integrating logic, dynamics, and constraints," *Automatica*, vol. 35, no. 3, pp. 407–427, 1999.

[27] T. Geyer, G. Papafotiou, and M. Morari, "Hybrid model predictive control of the step-down DC-DC converter," *IEEE Transactions on Control Systems Technology*, vol. 16, no. 6, pp. 1112–1124, 2008.

[28] X. Sun, C. Yuan, Y. Cai, S. Wang, and L. Chen, "Model predictive control of an air suspension system with damping multi-mode switching damper based on hybrid model," *Mechanical Systems and Signal Processing*, vol. 94, pp. 94–110, 2017.

[29] M. Kamelreiter, W. Kemmetmüller, and A. Kugi, "Digitally controlled electrorheological valves and their application in vehicle dampers," *Mechatronics*, vol. 22, no. 5, pp. 629–638, 2012.

[30] J. C. Ramos, A. Rivas, J. Biera, G. Sacramento, and J. A. Sala, "Development of a thermal model for automotive twin-tube shock absorbers," *Applied Thermal Engineering*, vol. 25, no. 11-12, pp. 1836–1853, 2005.

[31] A. K. Samantaray, "Modeling and analysis of preloaded liquid spring/damper shock absorbers," *Simulation Modelling Practice and Theory*, vol. 17, no. 1, pp. 309–325, 2009.

[32] C.-T. Lee and B.-Y. Moon, "Simulation and experimental validation of vehicle dynamic characteristics for displacement-sensitive shock absorber using fluid-flow modelling," *Mechanical Systems and Signal Processing*, vol. 20, no. 2, pp. 373–388, 2006.

[33] X. Sun, Y. Cai, S. Wang, Y. Liu, and L. Chen, "Design of a hybrid model predictive controller for the vehicle height adjustment system of an electronic air suspension," *Proceedings of the Institution of Mechanical Engineers, Part D: Journal of Automobile Engineering*, vol. 230, no. 11, pp. 1504–1520, 2016.

[34] A. Bemporad, G. Ferrari-Trecate, and M. Morari, "Observability and controllability of piecewise affine and hybrid systems," *IEEE Transactions on Automatic Control*, vol. 45, no. 10, pp. 1864–1876, 2000.

[35] F. D. Torrisi and A. Bemporad, "HYSDEL-A tool for generating computational hybrid models for analysis and synthesis problems," *IEEE Transactions on Control Systems Technology*, vol. 12, no. 2, pp. 235–249, 2004.

[36] F. Borrelli, A. Bemporad, M. Fodor, and D. Hrovat, "An MPC/hybrid system approach to traction control," *IEEE Transactions on Control Systems Technology*, vol. 14, no. 3, pp. 541–552, 2006.

[37] B. Hredzak, V. Agelidis, and M. Jang, "A model predictive control system for a hybrid battery-ultracapacitor power source," *IEEE Transactions on Power Electronics*, vol. 29, no. 3, pp. 1469–1479, 2016.

[38] O. König, G. Gregorčič, and S. Jakubek, "Model predictive control of a DC-DC converter for battery emulation," *Control Engineering Practice*, vol. 21, no. 4, pp. 428–440, 2013.

[39] K. Kobayashia and J. Imurab, "Deterministic finite automata representation for model predictive control of hybrid systems," *Journal of Process Control*, vol. 22, no. 22, pp. 1670–1680, 2012.

[40] A. Bempora, A. Garulli, S. Paoletti, and A. Vicino, "A bounded-error approach to piecewise affine system identification," *IEEE Transactions on Automatic Control*, vol. 50, no. 10, pp. 1567–1580, 2005.

[41] G. Trecate, E. Gallestey, P. Letizia et al., "Modeling and control of co-generation power plants: a hybrid system approach," *IEEE Transactions on Control System Technology*, vol. 12, no. 5, pp. 694–705, 2004.

[42] Y. Wang, S. Xie, and W. Wang, "Numerical simulation of cavitation performance of low specific speed centrifugal pump with slotted blades," *Journal of Drainage and Irrigation Machinery Engineering*, vol. 34, no. 3, pp. 210–215, 2016.

[43] Z. Wu, S. Chen, L. Yang, and B. Zhang, "Model of road roughness in time domain based on rational function," *Transactions of Beijing Institute of Technology*, vol. 29, no. 9, pp. 795–798, 2009.

[44] Z. Li, J. Huang, Y. Liu, and H. Jiang, "Modeling and simulation on white noise of road roughness in time domain," *Journal of Jiangsu University: Natural Science Editions*, vol. 37, no. 5, pp. 503–506, 2016.